Influence of surface plasmon propagation on leakage radiation microscopy imaging

Samuel Aberra Guebrou, J. Laverdant, Clémentine Symonds, S. Vignoli, François Bessueille, Joël Bellessa

Influence of surface plasmon propagation on leakage radiation microscopy imaging

S. Aberra Guebrou,[1,a)] J. Laverdant,[1] C. Symonds,[1] S. Vignoli,[1] F. Bessueille,[2] and J. Bellessa[1]
[1]*Université Claude Bernard Lyon 1 LPMCN, CNRS, UMR 5586, 69622 Villeurbanne, France*
[2]*Université Claude Bernard Lyon 1 ISA, CNRS, UMR 5280, 69622 Villeurbanne, France*

(Received 27 July 2012; accepted 4 September 2012; published online 18 September 2012)

We study in this Letter, the effect of the surface plasmon (SP) propagation and coherence on the images obtained by leakage radiation microscopy. The studied system is a set of nanocrystals deposited on a thin silver film supporting surface plasmon modes. More than 70% of the emission in this typical system comes from non-local emission. The diameter of the influence circle around the detection point is of the order of magnitude of the plasmon propagation length. We also present an original method to measure the propagation length (L_{spp}) of surface plasmons in complex systems by a two Young's slits experiment. This method can be useful for complex systems with a very short propagation length. © *2012 American Institute of Physics*. [http://dx.doi.org/10.1063/1.4753809]

The modification of the emitting properties induced by the proximity of a metallic surface has been largely investigated, since the pioneering work of Drexhage.[1] When the distance between an emitter and the metallic surface is smaller than 50 nm in the visible range, the main part of the emission is radiated into surface plasmon (SP) modes.[2] The radiation rate can be enhanced by several orders of magnitude in adequate conditions.[3,4] Alongside these studies, SP microscopy has been developed based on the high sensitivity of these modes.[5,6] This type of microscopy can be used to finely analyze surface modifications, with applications in biology and chemistry.[7–9] The fluorescence of nanoparticles near a metallic film can also be studied using leakage radiation microscopy (LRM).[10] This microscopy technique has the advantage of a luminescence enhancement by SPs, coupled to a high sensitivity to surface modifications. Nevertheless the interpretation of the resulting images has to take into account the propagating nature of surface plasmons. The spatial coherence induced by this extension has been evidenced by different methods,[11,12] but its direct influence on SP microscopy has never been studied.

The aim of this Letter is to study the influence of this predominant emission through SP mode on images obtained in leakage plasmon microscopy. The different contributions in the light observed at a given point of the image will be quantitatively studied showing the main contribution of a non-local emission. The radius of influence of the environment will be investigated using interference experiments allowing to explicitly check this non-local nature. We will also present a new method for measuring the plasmon propagation length, which could be useful for complex systems or systems with a short surface propagation length.

The experimental setup is depicted in Fig. 1(a). A classical LRM setup is coupled to a Young's slits experiment. A microscope objective focuses a 532 nm laser beam on top of the sample surface. The emission of the sample is then collected through the substrate with an oil-microscope objective (numerical aperture 1.49). A notch filter is placed on the detection path in order to remove the laser's wavelength. On channel I, direct space resolved images of the sample surface can be made (see Fig. 1(b)). On channel II, the Fourier plane (FP) of the microscope objective is imaged (FP) on the entrance slit of a spectrometer coupled to CCD detector giving direct dispersion relations of the sample (see Fig. 1(c)). Channel III is devoted to interference measurements. An image of the sample surface is made in an intermediate plane, in which are inserted V shaped Young's slits crossing a vertical one.[13] This system allows to extract the emission of two distinct regions of the sample to make them interfere on the entrance slit of the spectrometer.

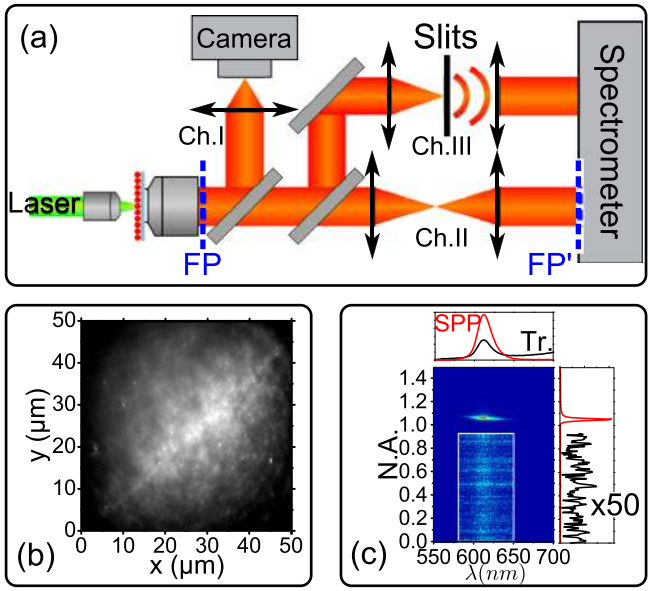

FIG. 1. Scheme of the experimental setup with 3 detection channels. Channel I is for real space images, Channel II for dispersion measurements, and Channel III for interference experiments. (b) Spatially resolved image of the sample surface emission collected with the setup and imaged on the CCD camera. (c) Spectrally resolved image of the FP of the microscope objective. The part inside the white rectangle is enhanced for clarity.

a)E-mail: samuel.aberra-guebrou@univ-lyon1.fr.

The sample studied consists in a set of CdSe nanocrystals (NCs) (Invitrogen™ Qdot® ITK™ Carboxyl Quantum Dots 605 conjugate) spin-coated on a 42 nm silver film thermally evaporated on a 150 μm glass coverslip substrate. The NCs' emission is in a linear regime with the laser intensity, and the distance between the NCs is smaller than the resolution of the setup. The NCs' concentration remains however far from the one leading to strong coupling regime with SPs.[14]

Fig. 1(b) shows a real space image of the sample emission collected with the LRM setup. In Fig. 1(c), shown is the corresponding spectral image of the FP, displaying the angular repartition of the sample's emission. The NCs' emission lies at 605 nm with a full width at half maximum of 25 nm. Two different contributions to the emission can be separated on the FP image: a dispersionless emission and a dispersive contribution. The dispersive contribution is a descending sharp line, which lies around $NA = 1.06$. The position of this bright line corresponds exactly to the plasmon dispersion line, and this emission is clearly the NCs' emission through the SP. The dispersionless part of the emission has no dependance with the angle and appears as a vertical band on the Fig. 1(c). Two phenomena can explain this contribution: the direct emission of the NCs through the silver film (the transmission of a 42 nm silver film is less than 5%) and the scattering of SP by the surface roughness. As the silver layer presents a very low roughness (1.6 nm measured on a 1 μm × 1 μm AFM image), contribution of scattering can be considered as negligible compared to the transparency.[15] On direct images (Fig. 1(b)), the dispersionless contribution is associated with a local behavior: at a given point, the collected light corresponds to the emission of the NCs located at this point; whereas the dispersive contribution is non local: at a given point, the dispersive emission is the leakage of propagating SP emitted by distant NCs from the detection point.[16]

A quantitative comparison can be made from Fig. 1(c). For a given angle, maximal intensity of the dispersive contribution is 100 times larger than the non-dispersive emission. Integrating the dispersive signal and the non-dispersive one shows that the SP signal collected by the setup corresponds to 70% of the total collected emission.

To confirm the predominant part of the non-local emission compared to the local emission, interferometric experiments have been performed. For this purpose, two slits are inserted in an image plane of the sample surface and select the emission of two regions of the sample. The interferences between the light coming from these regions are measured as a function of the wavelength and are shown on Fig. 2. Figure 2(a) corresponds to an excitation spot diameter of 10 μm, larger than the slits' separation ($\Delta = 5.4$ μm) on the sample. The fringes in this figure come from the surface plasmons emitted by the NCs, which illuminate coherently both slits. As shown in Ref. 13, the interference pattern in weak coupling can be interpreted as independent contributions of all the excited emitters, in this case, the NCs spread in the excitation spot. To understand the observed contrast (0.25 for Fig. 2(a)), two types of contributions to the interference pattern have to be separated: the NCs in between the slits which do not induce fringes and the NCs located on the side of the slits. The interference pattern generated by a NC located on the side of the slits does not depend on its position, as the phase difference only depends on the distance between the slits. Each NC generates the same interference pattern. Fig. 2(b) presents an interference pattern recorded with an excitation spot (diameter 1 μm) located on the side of the slits, showing well contrasted fringes. The visibility found in Fig. 2(b) is $\mathcal{V} = 0.75$ and corresponds to a SP propagation length of $L_{spp} = 3.4$ μm. This length deduced from the visibility is the same as the one directly measured with a cross section of the propagating SP intensity decay (top right of Fig. 2(b)).

The behavior is completely different for emitters located in between the slits. In this case the interference pattern is shifted when the NC position changes. If the distance between the emitters is larger than a few hundred nanometers (150 nm), the interference pattern is completely blurred. To illustrate this behavior, interference pattern with an excitation located in between the slits is shown on Fig. 2(c), where no fringes are present.

To modify the relative contribution of the central and lateral NCs, the spot size w has been varied, keeping the interslit distance constant.

The evolution of the fringes' visibility as a function of the gaussian shaped laser waist w varying from 1 to 30 μm (red dots) is displayed on Fig. 3. For small spot sizes, the visibility is low because the main part of the emitters contributing to the interference pattern is located in between the slits.

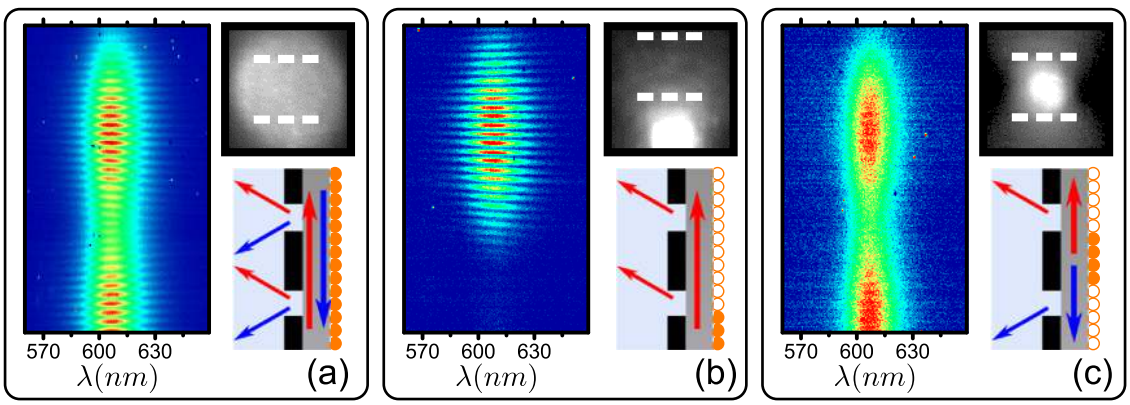

FIG. 2. (a) Spectrally resolved resulting interference pattern for a sum of emitters excited in between and on the sides of the two slits with an excited area of 10 μm. (b) Interferences recorded for a sum of emitters out of the slits. (c) Blurred interferences for a sum of independant emitters in between the slits.

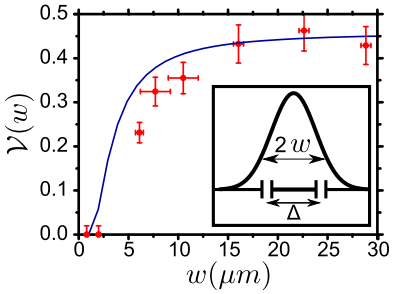

FIG. 3. Evolution of the fringes' visibility as a function of the spot size w (red dots). The inset sketches the laser shape on the sample surface with the selected region by the two slits. The blue line displays the calculated evolution of the visibility for a propagation length fixed at $L_{spp} = 3.3\,\mu$m.

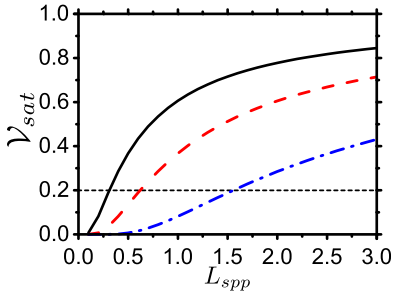

FIG. 4. Evolution of $\mathcal{V}_{sat}$ as function of L_{spp} for different distances Δ between the slits. $\Delta = 1\,\mu$m (black solid line), $\Delta = 2\,\mu$m (red dashed line), and $\Delta = 5\,\mu$m (blue dashed-dotted line).

When w increases, the contrast increases with the contribution of NCs on the side of the spot. At $w = 15\,\mu$m, the visibility reaches a maximum: for larger spot sizes, SPs emitted by the NCs located on the side do not propagate enough to reach the slits and modify the visibility. The saturation of this visibility curve gives the typical radius of influence of emitters in leakage radiation images: typically $15\,\mu$m in our case. These interference experiments show unambiguously that propagating modes have a major influence on the intensity detected in leakage radiation plasmon images. The intensity detected at a given point is influenced by emitters located on a ring of typical radius of the surface plasmon propagation length.

In order to confirm this experimental result, simulations have been performed. The emitters have the role to launch SPs with complex wavevectors. A gaussian shaped laser excites the emitters in a linear fluorescence regime. Two slits have been set in the center of the laser (inset of Fig. 3). The resulting intensity is obtained by adding the contributions of all the incoherent emitters. The results are displayed and superposed to the experimental ones in Fig. 3 and are in accordance using a SP propagation length of $3.3\,\mu$m.

For large excitation spots, the gaussian shape can be neglected and the intensity can be analytically calculated.[17] Supposing a constant illumination, the contribution of the different emitters is added. For emitters in between the slit, the contribution is constant, and for emitters on the side, the contribution is given by

$$I = I_0 e^{-2k''_{sp}d}(1 + e^{-2k''_{sp}\Delta} + 2e^{-k''_{sp}\Delta}\cos(k'_{sp}\Delta)), \qquad (1)$$

where d is the distance of an emitter from the first slit and Δ is the distance between the slits. The contrast of the fringes resulting from the sum of all the contributions is given by

$$\mathcal{V}_{sat} = \quad \exp(-k''_{sp}\Delta)\,. \qquad (2)$$

The analytical calculation gives a plasmon propagation length of $3.3\,\mu$m for $\mathcal{V}_{sat} = 0.44$, the same as the one obtained by numerical calculations and direct measurements on the propagation cross section of Fig. 2(b).

A remarkable point is that the propagation length can be simply deduced by the saturated visibility if the excitation spot is large enough. The measure of the saturated visibility can be used to directly access to the plasmon propagation length. To illustrate the dependance of the saturation value, we fixed the distance between the two slits and simulated the evolution of the saturated visibility of the fringes with the SP propagation length. The results are displayed Fig. 4. The chosen distance between the slits is larger than the diffraction limit of typical LRM setups (245 nm at 600 nm for a NA of 1.49). Considering an experimental limit for the visibility measurement of 0.2 (horizontal dashed line), propagation lengths as small as $0.2\,\mu$m can be measured for an interslit distance of $1\,\mu$m, the limit being $0.6\,\mu$m for $2\,\mu$m slits separation. Investigating the interference visibility is thus a very efficient way to measure SP propagation lengths particulary when this distance is small. Indeed, usual methods[10,18] based on direct measurement of the exponential decay of the intensity require a propagation length a least larger than the excitation spot.

In conclusion, we have investigated how the coherence behavior of surface plasmon modifies the images obtained by leakage radiation microscopy. We show that more than 70% of the detected intensity comes from non-local emission. The predominant contribution of delocalized plasmon has been confirmed with interference experiments showing that a ring with a typical radius of the plasmon propagation length contributes to the intensity detected at a given point of the image. Finally, we propose a method to investigate the propagation of surface plasmons. By illuminating a set of fluorescent emitters onto a flat surface, we are able to deduce the SP propagation length by a Young slits experiment. The fringes visibility tends to a saturation value directly related to the propagation length. This method can be easily extended to several systems such as semicontinuous films[19] and fractal plasmonics.[20]

[1]K. H. Drexhage, *Progress in Optics XII*, edited by E. Wolf (North Holland, Amsterdam, 1974).
[2]S. A. Maier, *Plasmonics, Fundamentals and Applications* (Springer, 2007).
[3]A. Neogi, C. W. Lee, H. O. Everitt, T. Kuroda, A. Tackeuchi, and E. Yablonovich, Phys. Rev. B **66**, 153305 (2002).
[4]C. Vion, P. Spinicelli, L. Coolen, C. Schwob, J. M. Frigerio, J.-P. Hermier, and A. Maitre, Opt. Express **18**, 7440–7455 (2010).
[5]W. L. Barnes, A. Dereux, and T. W. Ebbesen, Nature (London) **424**, 824–830 (2003).
[6]B. Rothenhausler and W. Knoll, Nature (London) **332**, 615–617 (1988).
[7]J. R. Lakowicz, Anal. Biochem. **298**, 1–24 (2001).
[8]J. R. Lakowicz, Plasmonics **1**, 5–33 (2006).
[9]C. Sonnichsen, B. M. Reinhard, J. Liphardt, and A. P. Alivisatos, Nat. Biotechnol. **23**(6), 741–745 (2005).

[10]A. Drezet, A. Hohenau, A. L. Stepanov, H. Ditlbacher, B. Steinberger, N. Galler, F. R. Aussenegg, A. Leitner, and J. R. Krenn, Appl. Phys. Lett. **89**, 091117 (2006).
[11]L. G. de Peralta, J. Opt. Soc. Am. B **27**, 1513–1517 (2010).
[12]S. Aberra Guebrou, J. Laverdant, C. Symonds, S. Vignoli, and J. Bellessa, Opt. Lett. **37**, 2139–2141 (2012).
[13]S. Aberra Guebrou, C. Symonds, E. Homeyer, J. C. Plenet, Y. N. Garstein, V. M. Agranovich, and J. Bellessa, Phys. Rev. Lett. **108**, 066401 (2012).
[14]D. E. Gomez, K. C. Vernon, P. Mulvaney, and T. J. Davis, Appl. Phys. Lett. **96**, 073108 (2010).
[15]A. Bouhelier and G. P. Wiederrecht, Phys. Rev. B **71**, 195406 (2005).
[16]D. G. Zhang, X. C. Yuan, A. Bouhelier, P. Wang, and H. Ming, Opt. Lett. **35**, 408–410 (2010).
[17]M. Born and E. Wolf, *Principles of Optics* (Pergamon, Oxford, 1980).
[18]P. Dawson, F. de Fornel, and J. P. Goudonnet, Phys. Rev. Lett. **72**, 2927 (1994).
[19]S. Buil, J. Aubineau, J. Laverdant, and X. Qulin, J. Appl. Phys. **100**, 063530 (2006).
[20]G. Volpe, G. Volpe, and R. Quidant, Opt. Express **19**, 3612–3618 (2011).